

Systematics of quadrupolar correlation energies

M. Bender,¹ G. F. Bertsch,¹ and P.-H. Heenen²

¹*Department of Physics and Institute for Nuclear Theory Box 351560, University of Washington, Seattle, WA 98195*

²*Service de Physique Nucléaire Théorique, Université Libre de Bruxelles, CP 229, B-1050 Brussels, Belgium*

(Dated: Oct. 5, 2004)

We calculate correlation energies associated with the quadrupolar shape degrees of freedom with a view to improving the self-consistent mean-field theory of nuclear binding energies. The Generator Coordinate Method is employed using mean-field wave functions and the Skyrme SLy4 interaction. Systematic results are presented for 605 even-even nuclei of known binding energies, going from mass $A=16$ up to the heaviest known. The correlation energies range from 0.5 to 6.0 MeV in magnitude and are rather smooth except for large variations at magic numbers and in light nuclei. Inclusion of these correlation energies in the calculated binding energy is found to improve two deficiencies of the Skyrme mean field theory. The pure mean field theory has an exaggerated shell effect at neutron magic numbers and addition of the correlation energies reduce it. The correlations also explain the phenomenon of mutually enhanced magicity, an interaction between neutron and proton shell effects that is not explicable in mean field theory.

PACS numbers: 21.60.Jz, 21.10.Dr

More than 3000 atomic nuclei with different combinations of proton number Z and neutron number N have been experimentally identified so far, and for about 2000 of them their masses, or, equivalently, their binding energies, have been measured [1]. This number is only a fraction (about 25%) of all the nuclei which are predicted to be bound, i.e. stable against nucleon emission. Since a large fraction of the unknown nuclei seems out of reach to be studied experimentally, an accurate theory of binding energies is needed. For example, one of the important motivations for studying nuclei far from stability is to better understand nucleosynthesis and the astrophysical environment in which it takes place [2]. In particular, the r-process of heavy-element production leaves an imprint of the binding energies of far-unstable nuclei on the mass abundances present today.

Among the theories of nuclear binding energy, the self-consistent mean-field theory [3] stands out as a fundamentally justified approach that is also computationally tractable over the entire mass table. Global calculations of binding energies are now available including both pairing and deformation effects in the mean field, using energy functionals of the nonrelativistic Skyrme form [4] or a relativistic mean-field model [5]. A systematic problem with such theories is an exaggeration of the increased binding at magic numbers, the shell effect. The accuracy of these pure mean field theories is of 1.5-2.0 MeV rms errors in binding energies [6], much poorer than that of more phenomenological approaches such as the Finite Range Liquid Droplet Model [7].

An obvious route to improve the theory is to include correlation effects. Indeed, this has already been done in a phenomenological way with good results [8, 9]. Some correlation effects can be subsumed in the parametrization of the mean-field energy functional, but not all. Most obviously, the rotational correlation energy of de-

formed nuclei is beyond mean-field theory, which can only describe the intrinsic state of a rotational band. The requirements on a theory of correlation energies are severe. Besides being computationally tractable, it must be systematic, applicable to both spherical and deformed nuclei. One approach, the RPA theory of correlation energies, has been applied recently to the binding energy problem by Baroni *et al.*, [10]. However, the RPA is not well convergent for short-range interactions, limiting its usefulness [11].

In this letter we report on global calculations of correlation energies in another well-defined theoretical extension of the mean-field approximation [12], based on the Generator Coordinate Method (GCM). The quadrupolar fluctuations about the mean-field solution are determined variationally by mixing configurations around the mean-field ground state. Our method includes also a projection on good angular momentum and particle number and applies to all nuclei irrespective of the shape characteristics of their ground states. It is thus systematic, which is an important criterion for constructing mass tables. It also satisfies the goal of including in the correlation energy, the rotational energy of deformed states.

The technical details of our calculation are as follows. The self-consistent mean-field equations are solved using the method presented in ref. [13]. Here the wave functions are represented on a triaxial 3-dimensional spatial grid, rather than in an oscillator basis as was done in ref. [4, 5]. The effective nucleon-nucleon interaction is an energy density functional of the Skyrme form; we have used the SLy4 parameter set [14]. This set was fitted to nuclear matter properties, nuclear charge radii, as well as binding energies of doubly magic nuclei. We also included a local pairing interaction of the form used in ref. [15], but with a reduced strength of $v_0 = -1000$ MeV fm³ to compensate the explicit correlations added by the

generator coordinate treatment[12].

The GCM has as ingredients a set of wave functions generated by constrained mean-field calculations and a Hamiltonian for calculating matrix elements among those configurations. The constraint that we use is the quadrupole operator $Q(r)$ and we minimize the function:

$$E[\phi] - \lambda \int d^3r \rho(r)Q(r). \quad (1)$$

Here ρ is the mass density and λ is a Lagrange multiplier adjusted to get a specific value of the quadrupole moment $q = \int d^3r \rho(r)Q(r)$. The value of q is positive for prolate and negative for oblate deformations. The choice of the configurations $|q\rangle$ is a computational issue that has to be carefully addressed for systematic calculations. If states are too closely spaced there is a large redundancy as well as an excessive computational cost. We have tailored our selection of configurations for a target accuracy of 0.2 MeV in the correlation energies. In ref. [16], it was found that this accuracy can be achieved when overlap probabilities of neighboring configurations is about 0.5 or higher, and we adopt that criterion here. We also restrict the deformations to shapes that have energies within 5 MeV of the mean-field ground state. Typically this gives $n_q = 7 - 20$ different configurations in our computational space [17].

There is an ambiguity in the choice of the Hamiltonian \hat{H} for use with a mean-field energy functional [18]. We use the so-called mixed density for the calculation of the density-dependent term in the Skyrme Hamiltonian, as is mostly done in the literature [19]. The GCM energy is the minimum of the expression

$$\frac{\langle \Psi | \hat{H} | \Psi \rangle}{\langle \Psi | \Psi \rangle}$$

where $|\Psi\rangle$ is an arbitrary state in the basis of the $|q\rangle$. The minimization is performed by solving the corresponding discretized Hill-Wheeler equations [20]. The orientation of the intrinsic deformed states $|q\rangle$ could be considered a continuous degree of freedom to be included in the minimization, but in practice we achieve the same result by projecting the intrinsic states on angular momentum zero when calculating matrix elements. The theoretical correlation energy is then obtained in two steps: we determine first the energy gain of an angular-momentum projected configuration $|q\rangle$ with respect to the mean-field minimum, $E_{J=0}$, and after that, the additional energy gained by mixing configurations with different q magnitudes, E_{HW} .

The needed matrix elements $\langle q|q'\rangle$ and $\langle q|\hat{H}|q'\rangle$ are calculated with the computer code described in ref. [12]. Besides performing the rotations to calculate the matrix elements needed for angular momentum projection, the code carries out a projection of the BCS wave function on good particle number N and Z . The number projection and the rotation operation are computationally

very demanding, and it was necessary to find additional computational shortcuts to make the global study feasible. One important savings was the use of a topological Gaussian overlap approximation which allows a two-point evaluation of the angular momentum projection integrals [17, 21]. The top-GOA was found to be quite adequate, except for very light nuclei, where a three-point approximation was sometimes needed. Another place where we made considerable computational savings was in the calculation of off-diagonal matrix elements in the $|q\rangle$ space. In principle, an n -dimensional basis requires the calculation of $n(n+1)/2$ overlaps and Hamiltonian matrix elements. These must be done explicitly for neighboring configurations, but matrix elements for more distant configurations can be estimated using another Gaussian Ansatz based on a measure of the separation between the configurations[16]. A tricky point arises in the mixing of weak prolate and oblate deformations which can have very high overlaps. We deal with this problem by defining a two-dimensional metric for calculating the separation of configurations as described in ref. [17]. With these approximations, the computational effort for the GCM minimization was reduced by 1 to 2 orders of magnitude, but still requiring on the order of 10^{17} floating point operations for the entire table of 605 nuclei.

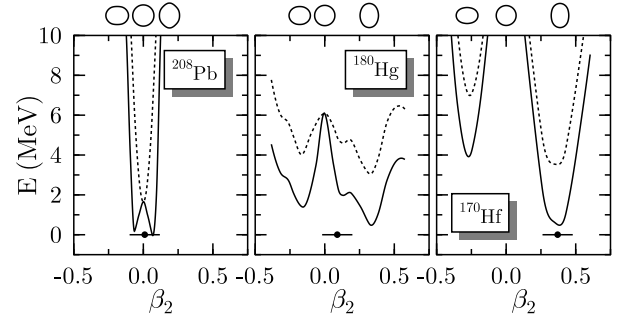


FIG. 1: Typical potential energy landscapes in the deformation coordinate. Shown are the curves for ^{208}Pb , ^{180}Hg , ^{170}Hf , representing a magic nucleus, a soft nucleus, and a deformed nucleus, respectively. See text for explanation.

We now present three calculations, typical of three different topologies. In Fig.1 are plotted the deformation energy curves of a doubly magic nucleus, ^{208}Pb , a statistically deformed nucleus ^{170}Hf , and a nucleus with oblate and prolate minima close in energy, ^{180}Hg . The configuration spaces used are given in Table 1. The ^{208}Pb is a very stiff nucleus, and only needed 4 configurations to achieve the target accuracy. In contrast, ^{180}Hg is a rather soft nucleus, and it required 15 configurations ranging from -20 b to +32 b to map out the accessible deformations. The mean-field potential energy landscapes for these three nuclei are shown as the dashed lines in Fig. 1.

One sees the narrow minimum at zero deformation for

TABLE I: Configuration spaces for typical heavy nuclei. Mass quadrupole moments q are given in units of barns. Oblate and prolate configurations are listed on separate lines.

| Nucleus | n_q | q values |
|-------------------|-------|----------------------------------|
| ^{208}Pb | 4 | -10 -5 |
| | | +5 +10 |
| ^{180}Hg | 15 | -20 -16 -14 -10 -6 -4 |
| | | +4 +6 +8 +12 +16 +20 +24 +28 +32 |
| ^{170}Hf | 12 | -20 -16 -13.75 -10 -5 |
| | | 5 +10 +15 +19.25 +22 +25 +30 |

TABLE II: Quadrupolar deformation and correlation energies of typical heavy nuclei. Energies are given in MeV.

| Nucleus | E_{def} | $E_{J=0}$ | E_{HW} | E_{corr} |
|-------------------|-----------|-----------|----------|------------|
| ^{208}Pb | 0.0 | -1.7 | 0.0 | -1.7 |
| ^{180}Hg | -3.0 | -2.5 | -0.5 | -3.1 |
| ^{170}Hf | -12.2 | -2.9 | -0.4 | -3.4 |

the magic ^{208}Pb , a much flatter potential energy surface for ^{180}Hg , and a surface with a strongly deformed minimum for ^{170}Hf . The energy gain from angular momentum projection is shown by the solid lines in the table. Obviously, there is no change for the spherical configurations but for finite $|q\rangle$ the projection lowers the energy below the mean-field value for every q . Even for ^{208}Pb , there is a net energy gain $E_{J=0}$ of the lowest projected energy with respect to the mean-field ground state. These numbers are given in Table 2.

The second step in our calculation is to apply the GCM to mix configurations with different values of q . The additional energy E_{HW} is given in Table 2 and shown as a dot in Fig. 1. The horizontal position of the dot indicates the average deformation of the mixed wave function (see [12] for its precise definition).

Our calculations include all but the lightest even-even nuclei for which the mass is known. The results presented in Fig. 2, are displayed as a function of neutron number N with isotopes connected by lines. On the top panel, we show the energy difference between the SLy4 mean-field theory and experiment[19]. Here the shell effect is very prominent at neutron numbers $N = 50, 82$, and 126 . The middle panel shows the calculated quadrupolar correlations energies. One sees that, for most nuclei, it is between 3 and 4 MeV, irrespective of whether the nucleus is spherical or deformed. However, near doubly magic nuclei, the correlation energy is much smaller. This difference has the right sign to mitigate the too-strong shell effect of the mean-field theory. The bottom panel in Fig. 2 shows the binding energies with and without inclusion of the correlation energy. There is a distinct improvement, but one sees that there remains some residual shell effect. Since we have only included the axial quadrupolar field, there could be significant correlation energies

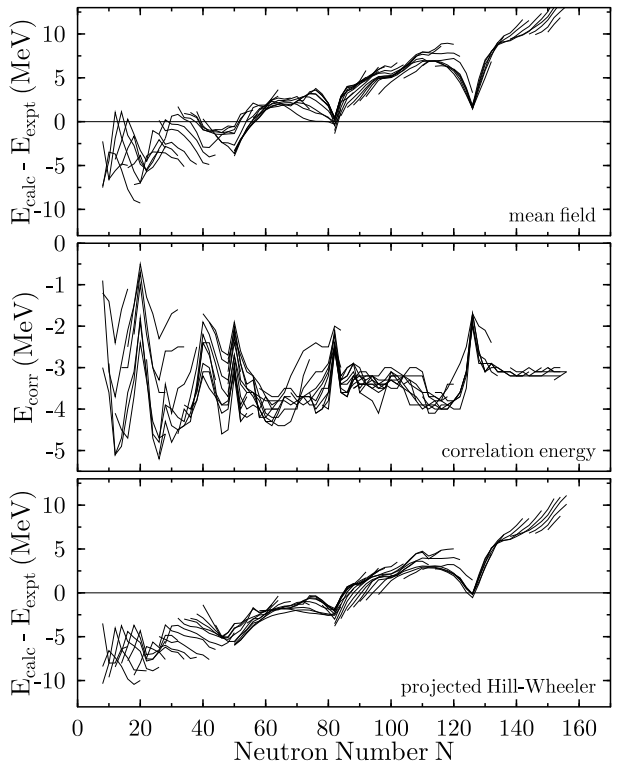


FIG. 2: Top panel: Difference of experimental and mean-field binding energies for the SLy4 interaction [4], as a function of neutron number with lines connecting isotopic chains. Middle panel: Theoretical quadrupolar correlation energies of the even-even nuclei. Note the expanded energy scale. Bottom panel: Difference of experimental and theoretical binding energies including the correlation energy. Comparison between binding energies obtained with and without the correlation contribution.

arising from other kinds of deformation or from pairing vibrations around closed shells[10]. Also, it is clear that a more complete theory requires a refitting of the energy functional to take into account the contribution from the correlation energy.

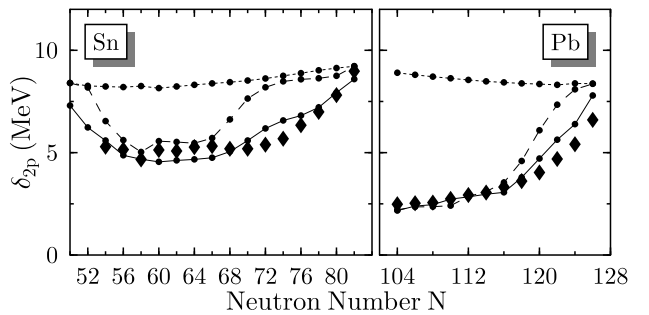


FIG. 3: Two-proton gaps for Pb and Sn isotopic chains.

A feature of the binding systematics that has been difficult to understand in mean-field theory is “mutually enhanced magicity” [23], the enhancement of shell effects

when both neutrons and protons form closed shells. This behavior can be seen in the neutron dependences of the two-proton gap, defined as

$$\delta_{2p}(N, Z) = E(N, Z-2) - 2E(N, Z) + E(N, Z+2). \quad (2)$$

In the independent-particle shell model, δ_{2p} is proportional to the difference between the Fermi energies of nuclei differing by two protons and thus it is a measure of shell gaps. This quantity is plotted in Fig. 3 for the $Z = 50$ (Sn) and $Z = 82$ (Pb) proton gaps, with the experimental points shown by black diamonds. There is clearly a reduction of δ_{2p} when going away from the doubly magic ^{132}Sn with 82 neutrons and doubly magic ^{208}Pb with 126 neutrons. Neglecting deformations, the mean-field prediction for δ_{2p} is quite flat, as shown by the short-dashed lines on the graphs. This reflects the independence of the single-particle proton gap on the neutrons in that approximation[26]. Allowing deformations in the mean-field energies already gives a change into the right direction, as shown by the long-dashed lines. The calculation including the full quadrupole correlation energy is shown by the solid lines. One sees that it brings the calculations even closer to experiment. The correlation energy thus provides a plausible explanation of mutually enhanced magicity. This conclusion is corroborated by a recent calculation of δ_{2p} in the Sn chain using the Bohr Hamiltonian, showing also the large improvement brought by quadrupolar correlations [24].

In conclusion, we find that quadrupole correlations beyond the mean field capture a significant part of the binding energy that is not describable in mean-field theory. We have shown that global calculations of these correlations are today feasible and could be incorporated in the future in the construction of effective interactions. Further improvements should be obtained by including other correlation effects related to octupole deformations or pairing vibration [10, 25]. Our basis does not contain triaxial shapes, but we do not believe they play as important a role. One of the major challenges which remains open is to include neutron-proton pairing effects, which may be responsible for the scatter of the residuals around the light $N = Z$ nuclei in Fig. 2.

This work is supported by the U.S. Dept. of Energy under Grant DE-FG02-00ER41132 and the Belgian Science Policy Office under contract PAI P5-07. The computations were performed at the National Energy Research Scientific Computing Center, supported by Department of Energy under Contract No. DE-AC03-76SF00098. PHH thanks the Institute for Nuclear Theory for hospitality where part of this work was carried out, and we also thank B. Sabbey for help.

<http://www-csnsm.in2p3.fr/AMDC/masstable/>
 Ame2003/mass.mas03.

- [2] K. Langanke and M. Wiescher, *Rep. Prog. Phys.* **64**, 1657 (2001).
- [3] M. Bender, P.-H. Heenen, and P.-G. Reinhard, *Rev. Mod. Phys.* **75**, 121 (2003).
- [4] M. V. Stoitsov, J. Dobaczewski, W. Nazarewicz, S. Pittel, and D. J. Dean, *Phys. Rev. C* **68**, 054312 (2003);
<http://www.fuw.edu.pl/~dobaczew/thodri/s9120v56.rev.txt>
- [5] G.A. Lalazissis, S. Raman, and P. Ring, *At. Data Nucl. Data Tables* **71**, 1 (1999).
- [6] G.F. Bertsch, B. Sabbey, and M. Uusnäkki, to be published.
- [7] P. Möller, J. R. Nix, W. D. Myers, and W. J. Swiatecki, *Atom. Data Nucl. Data Tables* **59**, 185 (1995).
- [8] F. Tondeur, S. Goriely, J. M. Pearson, and M. Onsi, *Phys. Rev.* **62** 024308 (2000).
- [9] S. Goriely, M. Samyn, M. Bender, and J. M. Pearson, *Phys. Rev. C* **68**, 054325 (2003).
- [10] S. Baroni, M. Armati, F. Barranco, R. A. Broglia, G. Colo', G. Gori, and E. Vigezzi, arXiv:nucl-th/0404019
- [11] I. Stetcu and C. Johnson, *Phys. Rev. C* **66**, 034301 (2002).
- [12] M. Bender and P.-H. Heenen, *Nucl. Phys.* **A713** (2003) 390; A. Valor, P.-H. Heenen and P. Bonche, *Nucl. Phys.* **A671** (2000) 145.
- [13] P. Bonche, H. Flocard, P.-H. Heenen, S. J. Krieger and M. S. Weiss, *Nucl. Phys.* **A443** (1985) 39.
- [14] E. Chabanat, P. Bonche, P. Haensel, J. Meyer, and R. Schaeffer, *Nucl. Phys.* **A635**, 231 (1998), *Nucl. Phys.* **A643**, 441(E) (1998).
- [15] C. Rigolet, P. Bonche, H. Flocard, and P.-H. Heenen, *Phys. Rev. C* **59**, 3120 (1999).
- [16] P. Bonche, et al., *Nucl. Phys.* **A510** 466 (1990).
- [17] M. Bender, G. F. Bertsch and P.-H. Heenen, *Phys. Rev. C* **69** (2004) 034340.
- [18] T. Duguet and P. Bonche, *Phys. Rev. C* **67** 054308 (2003).
- [19] We also omit some small terms that appear in the Hamiltonian formulation of the Skyrme interaction but not in the energy density functional.
- [20] D. L. Hill and J. A. Wheeler, *Phys. Rev.* **89** (1953) 1102; J. J. Griffin and J. A. Wheeler, *Phys. Rev.* **108**, 311 (1957).
- [21] K. Hagino, P.-G. Reinhard, and G. F. Bertsch, *Phys. Rev. C* **65**, 064320 (2002).
- [22] Since the SLy4 interaction was fitted to only magic nuclei, the other nuclei show a trend of increasing residuals with mass number. This is easily removed by a minor adjustment of parameters.
- [23] D. Lunney, J. M. Pearson, and C. Thibault, *Rev. Mod. Phys.* **75**, 1021 (2003).
- [24] P. Fleischer, et al., ArXiv:nucl-th/0408032 (2004).
- [25] P.-H. Heenen, et al., *Eur. Phys. J. A* **11** 393 (2001).
- [26] M. Bender, et al., *Eur. Phys. J. A* **14** 23 (2002).

[1] G. Audi, A. H. Wapstra, and C. Thibault, *Nucl. Phys.* **A729**, 337 (2003); the data file is available at